Binary Offset Carrier (BOC) and Binary Phase Shift Keying (BPSK) Modulation in indoor Drones GNSS Recievers using Multipath Error Envelope MEE Technique

*Ahmad Alhosban**

Amman Arab Univesity, Assistant Professor of Avionics, Faculty of Avaition, Amman, Jordan *ahmad_alhosban@yahoo.com*

Abstracts: The applications of unmanned aerial vehicles (UAVs) have greatly eased the lives of human being. Due to the mass commerial production of UAVs (or Drones) and the support of the ongoing scientific research, it can now be used in disaster monitoring, surviellance, fire conrolling and many outdoor usages. However, the indoor applications have stricter requirements for the autonomous positioning capability of UAVs, requiring its positioning accuracy to be within the narrower areas and aisles. The Global Navigation Satellite System (GNSS) is currently the only guidance and autorecovery method that can be applied directly and consistently to UAV positioning. The current GPS L1C and/or Galileo E1 open services signals are being widely used for this purpose. Moreover, the Binary Offset Carrier (BOC) techniques have been recently adopted in Galileo and GPS BIII as one of the efficient mitigation methods to decrease the interference/multipath delays and to increase both the Position Accuracy and the immunity of GNSS interferences. This research aims to present a software method of assessing the improvements of the Accuracy, and yet the Availability, by producing the MEE for BOC technique. The used methodology is analyzing the theoretical equations behind the interfernece multipath error envelopes in both BPSK and the new BOC signals. The Results show a higher performance of BOC GNSS Recievers over BPSK ones, and less delay.

Keywords: GNSS; GPS, Drones; BPSK, BOC; MEE.

1. INTRODUCTION

The first Binary Phase Shift Keying (BPSK) GNSS version of GNSS recievers were used in GBAS CAT I performance - so called GNSS landing system (GLS), and it was certified in 2002 by the International Civil Aviation Organization (ICAO) as per fully technically detailed in both [1] and [2], It was after the Selectivity Availability (SA) had been removed in May 2001, then after, many systems were deployed in CAT I performance and had been operated successfully in France, Germany and USA using the GPS signal in space or GLONASS Russian Systems since 2002. The worldwide research had continued for achieving CAT II performance certification since that time until it has been recently approved in Nov 2020 using GPS single constellation [3], and it still under foreseen for CAT III (or what newly called GAST-F), the latest performance of CAT III is tended to be achieved only and if only dual constellation is being used by adding European Galileo constellation.

A previous study [4] showed that the assumption of having dual constellation is subjected to the evaluation of certain factors, such as: firstly, the delay in time due to phase measurements during phase combination at the receiving antenna, which might cause minimizing the accuracy of the PNT information or/and minimizing the margin below the stringent Vertical Alert Limits (VAL) in the integrity availability. Secondly, the complexity of using the multichannel receivers can also cause further delay in time. And thirdly, above of all, for political reasons, depending on nation own GNSS constellation would add a significant value of independency in terms of Politics, Economics and Security as per fully detailed in Ref [5]. On the other hand, President of the United States of America has recently signed a new Executive Order on Position, Navigation and Timing (PNT) services in Feb. 2020, encouraging the development of a resilient PNT infrastructure that isn't exclusively reliant on the Global Positioning System (GPS) of satellites, its aim is motivating all providers to search for alternatives of such critical infrastructure [6]. However, the indoor applications have stricter requirements for the autonomous positioning capability of UAVs, requiring its positioning accuracy to be within the narrower areas and aisles. The Global Navigation Satellite System (GNSS) is currently the only guidance and autorecovery method that can be applied directly and consistently to UAV positioning[17].

The main aim of this paper was made to examine the using of a Single Constellation (SC) in GBAS Landing Systems, particularly Galileo system. In which the Multipath error is considered a limiting factor to achieve the needed performance to meet the CAT II/III requirements in terms of Accuracy and yet availability. On the other hand, the BOC signals showed a better anti-multipath and anti-interference over the BPSK, in terms of better MEE. The generic BOC modulation has been adopted in the modernized Global Positioning System (GPS) [7] and the European Galileo System [8], because of its good spectral isolation from heritage signals, high accuracy, multipath interference resistance compared with BPSK modulation. Furthermore, and yet, the Multiplexed BOC (MBOC) modulation has been used for the Galileo E1-B/C and GPS L1C (frequency (1575.42 MHz) signals to achieve enhanced accuracy and multipath interference resistance by using multilevel subcarrier symbols or combining different subcarrier symbols.

Recently, a new proposed Frequency-Hopping BOC (FH-BOC) scheme as per Jian gang et all, in 2020, [9] might improve the anti-interference performance and mitigates the ACF ambiguity problem of BOC modulation, the proposed FH-BOC modulation combines the most two practical and dominant spread spectrum techniques; the direct-sequence spread spectrum (DSSS) and the frequency-hopping spread spectrum (FHSS) techniques. because the acquisition time and complexity of the receiving process for the proposed FH-BOC signal are the same for the BOC signal with the same Main Lobe Bandwidth MLB. This new proposed modulation may be used as a new technique for the next-generation GNSS signal design, especially military signal design, but it is not used to yet, and needed to be deeply experimented as well. Furthermore, another new technique for MBOC is also proposed by Xin et all, in 2021, [10], called MBOC-POS, where the subcarrier periodic shifting binary offset carrier modulation is used as the lower-order component instead of sine binary offset carrier modulations. In which, different proposed implementations of MBOCPOS modulations were compared with traditional multiplexed binary offset carrier (MBOC) signals in multipath mitigation, tracking accuracy, anti-interference and compatibility. Then, resulted in reduction of 35% of the multipath error envelope MEE is with the filter bandwidth of 10 MHz, also, it said that it may be used as a new option for MBOC modulations in next-generation signal design. But it should be subjected to a common test tool for examining its efficiency in terms of MEE envelope.

The results showed that the chip spacing and the relative amplitude are the key factors in multipath mitigation in the code tracking loop, but the relative amplitude is the key factor in decreasing the multipath error in the phase tracking error. Moreover, in terms of the multipath error, the BOC (2,2) modulations has the best performance among all, BOC (1,1) has better performance than the currently used BPSK. More results can be found for other new schemes that would be used in the future new signal generations.

2. PROBLEMATIC ANALYSIS OF THE INTERFERENCE/MULTIPATH ERROR

In general, Multipath is the propagation phenomenon that results in radio signals reaching the receiving antenna by two or more paths; this could affect the original signal in constructive (when the reflected phase angle is 0) or destructive (when the reflected phase angle is 180), However, interference in terms of amplitude varying and/or phase shifting. This interference can be formulated intentionally or unintentionally. The intentionally cause is considered as a spoofing in the Electronic Warfare (EW), this Electronic Attack has been approved in [11] that there is an Analogy of interference of signals at the Receiving Antenna and inside Receiver Signal processing from one side, and Multipath interference from the other side. Basically, the causes of the unintentionally multipath could be mainly reflection wise or/and diffraction wise in both specular and diffuse, the reflection and the diffraction are generated by the existing of the obstacles nearby the receiving antenna. However, there are two important assumptions underlying most GNSS-receiver multipath mitigation Approaches: firstly, is the Multipath components are being delayed relative to the direct path signal, because they have to travel a longer distance, and secondly is the Multipath signals are being weaker than the direct path signal, since some power will be lost due to the reflection. So the accumulated signal at the receiving antenna can be given by the following equation 1:

$$r(t) = \underbrace{A_0 . d(t-\tau_0).c(t-\tau_0).\cos(2\pi f_{L1} t - \theta_0)}_{\text{LOS/Direct signal}} + \underbrace{A_1 . d(t-\tau_1).c(t-\tau_1).\cos(2\pi f_{L1} t - \theta_1)}_{\text{Reflected signal}} \quad (1)$$

Where:

$r(t)$ is the received GPS signal at the antenna.

A_o, τ_o, θ_o : are the amplitude , the propagation delay, and the carrier phase shift respectively of the direct signal. And A_1, τ_1, θ_1 : are for the one reflected multipath signal. The phase rate of change is assumed to be zero, and The delay of the ground reflection is a dependent factor on the altitude of the aircraft (user) antenna and the elevation angle is given by the following equation 2 below [12]:

D= 2. h. Sin (elev.) (2)

Where D is the delay of the ground reflection, h is the altitude of the aircraft antenna, and elev. is the elevation angle. After Matlab simulation, the resultant signal will be analyzed inside the receiver, it will be auto correlated then entered the discriminator, the discriminator will be affected in all the above parameters, figure 1 below shows the affected discriminator my multipath.

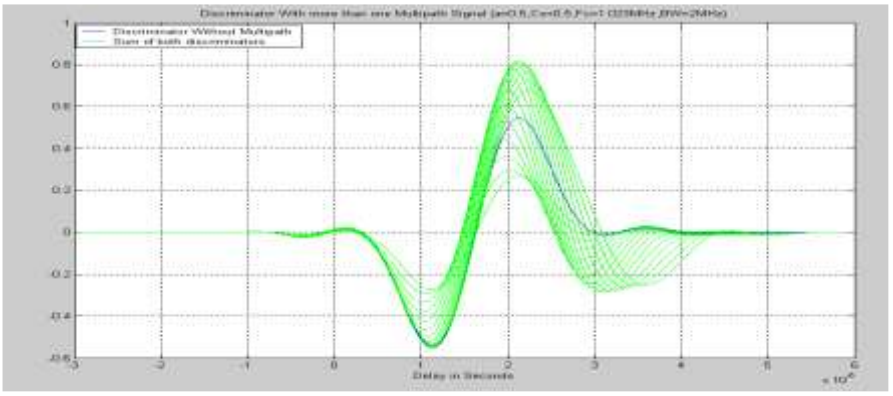

Figure 1. Discriminator affected by multipath [edited by Authors]

On the other hand, Mitigation methods could be classified to the following three types: Receiver-based mitigation methods, Antenna-based mitigation methods and Sitting-based mitigation methods. The first two methods could be applied for both the User (aircraft) receivers, and the Ground stations receivers. However, some classifications refer to the hardware and software-based mitigation methods also, they are located in the domain of Receiver-based methods. The sitting-based method would be applied to the ground station receivers only in GBAS application, due to the mobility of the aircraft, where the antennas are already sited once in the structure of the aircraft, and almost no control on the aircraft movement during the last phase of flight. In the same manner, the landing aircraft will be in a stable position with respect to the constellation space segments and what's needed is only the best position of the antenna in the aircraft structure, a lot of studies have investigated this point deeply and they have a satisfied results in mitigating the effect of the aircraft structure in terms of multipath, Upon these mitigation methods, it can be said that the multipath phenomena could be classified also to two types: the User multipath (mobile user i.e. aircrafts), and Ground station receiver's multipath, it can be resembled by the Ground Accuracy Designator (GAD).

Concerning the antenna-based and the sitting-based mitigation methods, they need to be experimentally dependent, improvement jumps are little and short in this aspect, but the Last two types of Chock ring and MLA (Multipath Limiting Antenna) could improve the performance of the Ground stations in GBAS stations from GAD letter A to better B or C letters. researches fulfilled this domain [13], [14], particularly [15], it compared the following antenna array types, each of them was assumed to have 7 antenna elements: Flat Antenna Array, Curved Antenna Array. Stack Antenna Array, and Curved (B) Antenna Array. In which, the results of this research approved, based on the simulation results, that the 3-D antenna array (7 elements) had the best multipath rejection performance in both the horizontal and vertical dimensions. Most importantly, and related to this research the focus will be on the Receiver-Based Mitigation Methods in the next section.

3. RECEIVER-BASED MITIGATION METHODS – MULTIPLEXED BINARY OFFSET CARRIER (MBOC)

In general, the receiver-based mitigation methods are those techniques used to reduce the multipath effect using the signal processing methods inside the receiver, specifically the ways implemented to enhance the performance of the tracking loops. However, there are two methods: The Correlator Techniques and the Signal Structure Techniques, our MBOC modulation technique is located under the signal structure technique, but it is strongly linked with the correlator technique after the signal comes in from the front end to the signal processor /tracking channels in the GNSS receivers, thus, both of them will be analyzed in this section in order to build up the MEE software.

Conceptually, The Binary Offset Carrier (BOC) means to form the spectral shape (power distribution over frequency) of a transmitted signal. BOC type signals are usually expressed in the form BOC (f_{shift}, f_{chip}) where frequencies are indicated as integer multiples of the GPS C/A Code chip rate of 1.023 M_{cps}. For example, a BOC (10, 5) signal has actually a sub-carrier frequency of 10 x 1.023 MHz = 10.230 MHz and a code chip rate of 5 x 1.023MHz = 5.115 MHz, the ratio of the 2x f_{shift}/f_{chip} is the n ratio which could be even or odd, this n number is one of the factors that contribute inside the equation of signal itself as it will be mentioned in the next section. Figure 2-left panel below shows the two modulation schemes and how the power is spread over the frequencies, and figure 2-right panel shows its effect in the Autocorrelation Function ACF. Thus, the key parameter of a signal structure with respect to multipath is the signal bandwidth, because large bandwidth leads to a small amplitude of the multipath error.

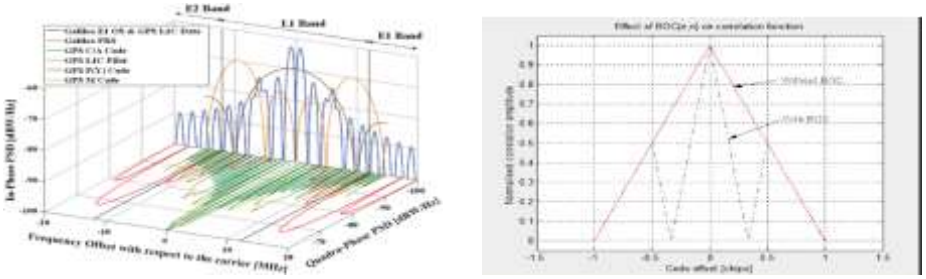

Figure 2. Left panel: New Modern GNSS signal structure [16], right panel: Effect on the Autocorrelation Function ACF [Edited by the Author]

However, the Multiplexed BOC (MBOC) is a new design, it introduces the multiplexed binary offset carrier (MBOC) spreading modulation recently recommended by the GPS-Galileo Working Group on Interoperability and Compatibility for adoption by Europe's Galileo program for it Open Service (OS) signal at L1 frequency, and also by the United States for its modernized GPS L1 Civil (L1C) signal. Its idea is based on various investigations that may be led to candidates for a L1 Open Service optimized signal structure which is called a CBCS solution also (Composite Binary Coded Symbols). It can be expressed by a superposition of BOC (1,1) and a BCS (Binary Coded Symbol) waveform with the same chip rate, equation 3 below:

$$CBCS = \propto . BOC(1,1) + \beta . BCS(n,1) \quad (3)$$

where α and β are values in percentage (%) under the condition α + β =100 %, and n represents the number of symbols. However, the BCS signal is a generalization of the BPSK-R and BOC modulation (except for BOC (k*n/2, n) with k odd) in both the sine and cosine versions. Thus, the well-known BPSK and BOC modulations can be understood as a particular case of the BCS modulation. for more information, [ION GNSS 18th, Hein, Jose-Angel Avila Rodriguez]. Both BOC and MBOC had enhanced the Multipath Error Envelope delay dramatically from 250-300 meters in BPSK down to less than 10 meters in MBOC and less than 50meters in BOC, figure 3 below, where the black colored curve is BOC (2,2), the red is BOC (14,2), and the blue is BPSK (1), but with some drawbacks; a larger bandwidth for BOC signals is still needed with comparison the BPSK, this may reach 32 MHz, and may be impact the design of the receivers.

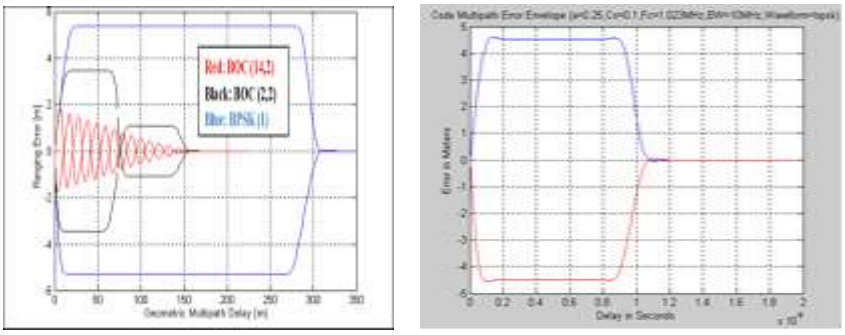

Figure 3. Effect of BOC and BPSK on the Multipath Error Envelope MEE [17, edited by authors]

4. MBOC AND MEE THEORETICAL SIGNAL PROCESSING INSIDE THE GPS RECEIVER

In order to produce formula of both phase and code error envelopes, first, we processed the accumulated signal at the front end of the global general GPS receiver architecture shown in Figure 4 below in a simple way that serves this goal.

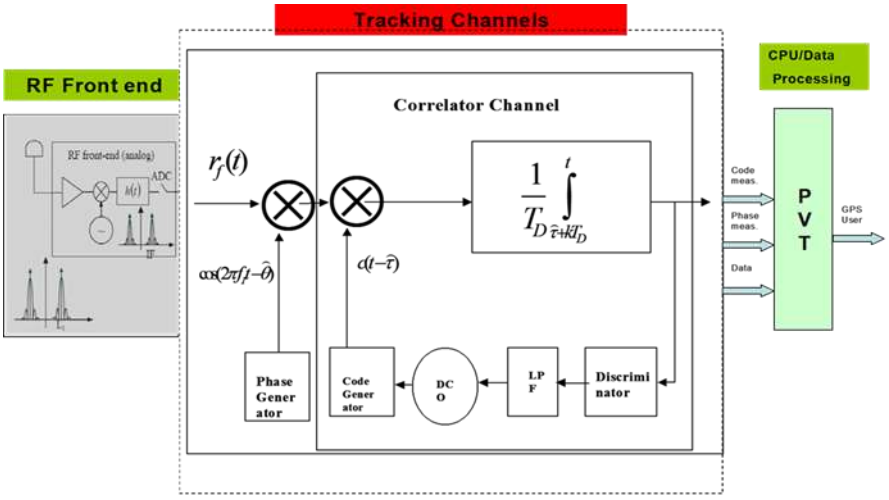

Figure 4 Block Diagram for General GNSS Receiver [edited by Authors]

The receiver consists of three main parts: the front end, the tracking channels and the PVT solution to the user. In the front end part, the functions of Analog to digital converting (ADC), Sampling, Encoding, and the Selective Filtering (h(t)) is taking place. The input of this stage is the GPS received signal from each satellite in view through the antenna, as seen in Equation 4 below:

$$r(t) = A.d(t-\tau).c(t-\tau).\cos(2\pi f_{L1}t - \theta) + n(t) \qquad (4)$$

Where $r(t)$ is the received GPS signal, A is the amplitude of the received signal, d(t) is the GPS navigation message, c(t) is the Gold spreading code, τ is the propagation delay, θ is the carrier phase shift, includes the Doppler effect , and the n(t) is the white Gaussian noise.

In the presence of the multipath error, the GPS received signal will be as follows under the assumption of one reflected ray and neglecting the noise (noiseless channel) as a first approximation as seen in Equation 5 below again: $r(t) = A_o.d(t-\tau_o).c(t-\tau_o).\cos(2\pi f_{L1}t-\theta_o) + A_1.d(t-\tau_1).c(t-\tau_1).\cos(2\pi f_{L1}t-\theta_1)$ (5)

LOS/Direct signal Reflected /interfering signal

Where: $r(t)$ is the received GPS signal at the antenna, A_o, τ_o, θ_o : are the amplitude, the propagation delay, and the carrier phase shift respectively of the direct signal. And A_1, τ_1, θ_1 are for the one reflected multipath signal. The output of the RF front end is the same signal but filtered and sampled, under the assumption of neglecting the quantization errors as seen in equation 6 below.

$$r(t) = A_o.d(t-\tau_o).c_f(t-\tau_o).\cos(2\pi f_l t - \theta_o) + A_1.d(t-\tau_1).c_f(t-\tau_1).\cos(2\pi f_l t - \theta_1) \quad (6)$$

Where the small (*f*) denotes the filtered signal and the (*I*) denotes the Intermediate Frequency (IF) frequency conversion. The front stage is not simulated by the produced program, neither the last stage which the data processing unit that finalized the navigation solution (PVT: Position, Velocity, and Time) in its readable form by the user. The only simulated stage is the tracking channels. Equation 6 above is the input to the tracking channels (Auto Correlator Function ACF), which consists of the following circuitry:

- Carrier Tracking Loop (PLL/FLL): to generate an instantaneous carrier replica of the incoming signal.
- Code Tracking Loop: (DLL) to generate an instantaneous code replica of the incoming signal, it could be coherent or non-coherent with phase tracking loop. The most frequent architecture is FLL (if the phase pseudo range measurement is not needed), because it's more robust, and the non-coherent DLL loop. DLL loops generates usually the early and the late autocorrelation functions; in this case a discriminator is needed.
- Discriminator: it has the function of generating the error voltage produced by the early and late correlators with different ways (could be differencing or multiplying) this error voltage drives the DCO, the Differential Controlled Oscillator to generate the difference in phase or code error that compensates the errors in the loop by iterative process.
- Low Pass Filter: is needed to get rid of the unwanted generated frequencies due to the autocorrelation functions.

Integrator: is accumulating the power in the spread GPS incoming signal each time of the loop process and over the interval of the 1ms (the navigation message period).

4.1. Costas PLL /Phase Tracking Interfering/Multipath Error

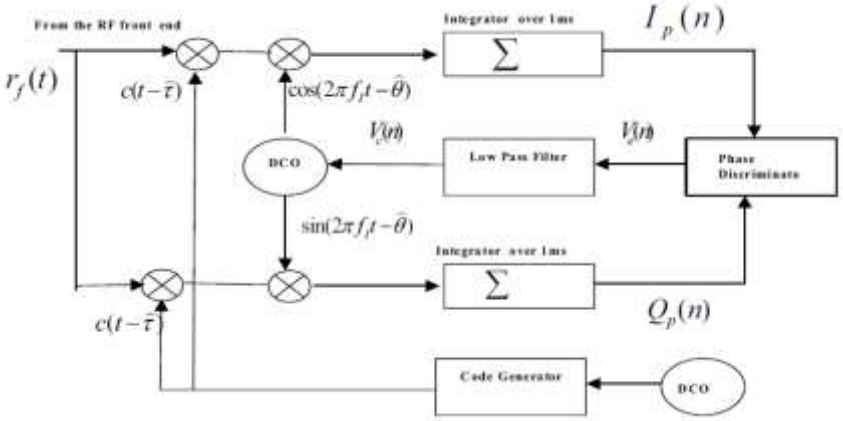

Figure 5. Costas PLL Loop

As a first step we can consider the PLL is not locked, that incoming phase is not the same as the estimated phase in the Costas PLL loop shown in Figure 5 above, the input signal is Equation 6 above with the multipath error embedded in it.

Where $t = kT_D$, then;

$$r(t) = A_o.d(kT_D - \tau_o).c_f(kT_D - \tau_o).\cos(2\pi f_l kT_D - \theta_o) + A_1.d(kT_D - \tau_1).c_f(kT_D - \tau_1).\cos(2\pi f_l kT_D - \theta_1) \quad (7)$$

$$\theta - \hat{\theta} = K_{DCO} \int_0^t V_c(v)\,dv \quad (8)$$

The phase is the integration of the DCO command voltage.

$$I_p(n) = {}^{A}/_{2}.d(n).K_c(\tau - \hat{\tau_o}).\cos(\theta - \hat{\theta_o}) + \alpha.{}^{A}/_{2}.d(n).K_c(\tau - \hat{\tau_1} + \Delta\tau).\cos(\theta - \hat{\theta_1} + \Delta\theta) \quad (9)$$

$$Q_p(n) = {}^{A}/_{2}.d(n).K_c(\tau - \hat{\tau_o}).\sin(\theta - \hat{\theta_o}) + \alpha.{}^{A}/_{2}.d(n).K_c(\tau - \hat{\tau_1} + \Delta\tau).\sin(\theta - \hat{\theta_1} + \Delta\theta) \quad (10)$$

Where:

$K_c(\tau - \hat{\tau_o})$ is the autocorrelation function of the in-phase /Quadrature-phase of the LOS signal.

$K_c(\tau - \hat{\tau_1} + \Delta\tau)$ is the autocorrelation function of the in-phase /Quadrature-phase of the reflected signal.

$\Delta\tau$ is the time delay due to multipath

$\Delta\theta$ is the phase delay due to multipath, assuming negligible Doppler Effect

The phase discriminator could be either: Product or Costas discriminator, Arc tangent Discriminator, or 4-quadrant discriminator. In the Product or Costas Discriminator;

$$V_e(n) = I_p(n).Q_p(n) \quad (11)$$

$$V_e(n) = {}^{A^2}/_{4}.K^2(\tau - \hat{\tau_o}).\sin(\theta - \hat{\theta_o}).\cos(\theta - \hat{\theta_o}) \quad (12)$$

When the loop is locked; $\theta - \hat{\theta_o} = 0\ (\pi)$

$$V_e(n) = {}^{A^4}/_{8}.K^2(\tau - \hat{\tau_o}).\sin(2(\theta - \hat{\theta_o})) \quad (13)$$

So, the discriminator is not linear and not normalized and with ambiguity of π, it can be normalized by dividing the last output by the power of the both punctual correlators:

$$V_e(n) = \frac{I_p(n).Q_p(n)}{(I_p^2(n)+Q_p^2(n)} \quad (14)$$

$V_e(n) = {}^{1}/_{2}.\sin(2(\theta - \hat{\theta_o}))$ normalized (15)

For the 4-quadrant Discriminator: $V_e(n) = \arctan(2.Q_p(n).I_p(n))$, The ambiguity of π is removed.

For the Arctangent Discriminator:

$$V_e(n) = \arctan\left(\frac{Q_p(n)}{I_p(n)}\right) \quad (16)$$

$$V_e(n) = (\theta - \hat{\theta_o})(n) \quad (17)$$

Which is normalized and linear but still with ambiguity of π. Finally, it was fully demonstrated that the phase tracking error due multipath is:

$$\varepsilon_\theta = \theta - \hat{\theta}_\circ = \arctan\left[\frac{\alpha.K_c(\tau_\circ - \hat{\tau}_\circ + \Delta\tau).\sin(\Delta\theta_1)}{K_c(\tau_\circ - \hat{\tau}_\circ) + \alpha.K_c(\tau_\circ - \hat{\tau}_\circ + \Delta\tau).\cos(\Delta\theta_1)}\right] \text{ Eq.} \quad (18)$$

And the last equation, Eq. (18), was used in the Matlab program to be simulated with company of the equations that are needed in the following section.

4.2. Non-coherent DLL/Code Tracking Interfering / Multipath Error

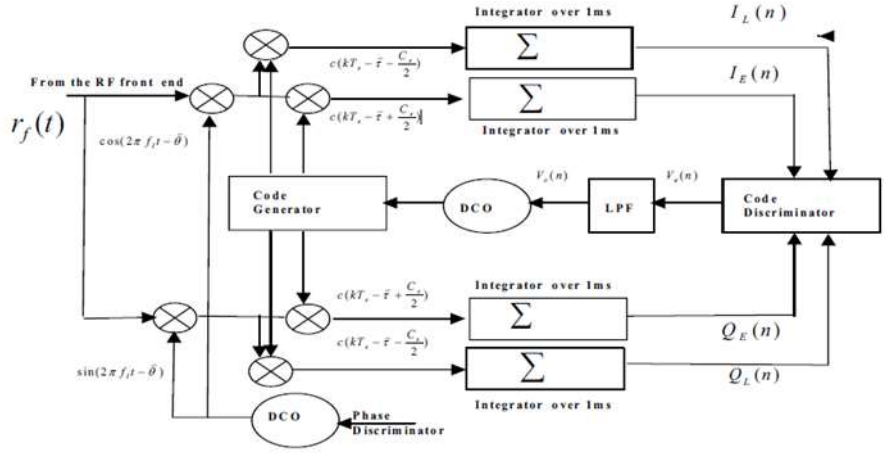

Figure 6. Non coherent DLL loop [edited by Authors]

$$I_L(n) = {}^{A}/_{2}.d(n).K_c(\varepsilon_\tau - C_s/2).cos(\varepsilon_\theta) + \alpha.{}^{A}/_{2}.d(n).K_c(\varepsilon_\tau - C_s/2 + \Delta\tau).cos(\varepsilon_\theta + \Delta\theta)$$

$$I_E(n) = {}^{A}/_{2}.d(n).K_c(\varepsilon_\tau + C_s/2).\cos(\varepsilon_\theta) + \alpha.{}^{A}/_{2}.d(n).K_c(\varepsilon_\tau + C_s/2 + \Delta\tau).\cos(\varepsilon_\theta + \Delta\theta)$$

$$Q_L(n) = {}^{A}/_{2}.d(n).K_c(\varepsilon_\tau - C_s/2).\sin(\varepsilon_\theta) + \alpha.{}^{A}/_{2}.d(n).K_c(\varepsilon_\tau - C_s/2 + \Delta\tau).\sin(\varepsilon_\theta + \Delta\theta)$$

$$Q_E(n) = {}^{A}/_{2}.d(n).K_c(\varepsilon_\tau + C_s/2).\sin(\varepsilon_\theta) + \alpha.{}^{A}/_{2}.d(n).K_c(\varepsilon_\tau + C_s/2 + \Delta\tau).\sin(\varepsilon_\theta + \Delta\theta)$$

LOS/Direct signal — One reflected signal

Where:

$\varepsilon_\tau = \tau_0 - \hat{\tau}$ is the LOS code tracking error

$\varepsilon_\theta = \theta_0 - \hat{\theta}$ is the LOS phase tracking error

$\Delta\tau = \tau_1 - \tau_0$ is the code tracking error due to multipath

$\Delta\theta = \theta_1 - \theta_0$ is the phase tracking error due to multipath

τ_0, θ_0 are for the LOS direct signal

τ_1, θ_1 are for the reflected multipath signal

The second part of the equations represent the multipath contribution to the early late correlator, and her we have two types of discriminators: The Dot-Product discriminator, and the early minus late power discriminator one, in the dot-product one, which won't be used in the program this time, its resultant output signal is:

$$V_e(n) = I_p(n).\left(I_E(n) - I_L(n)\right) + Q_p.(Q_E(n) - Q_L(n)) \quad (20)$$

But for the Early- minus- late discriminator:

$$V_e(n) = \left(I_E^2(n) + Q_E^2(n)\right) - (I_L^2(n) + Q_L^2(n)) \quad (21)$$

$$V_e(n) = {}^{A^2}/_{4}.\left(K^2(\varepsilon_\tau + C/2) - K^2(\varepsilon_\tau - C/2)\right) + \alpha^2.{}^{A^2}/_{4}.(K^2(\varepsilon_\tau + C/2 + \Delta\tau) - K^2(\varepsilon_\tau - C/2 + \Delta\tau)) \quad (22)$$

As an approximation, we will consider no effect due to filter on the correlation function, it can be offset if its delay time has been known.

So, $K_{cf} = K_c$, And then,

$$K_c(\varepsilon_\tau) = \begin{cases} K_c(\varepsilon_\tau) = 1 - \frac{|\varepsilon_\tau|}{T_c}, \ if\ |\varepsilon_\tau| \ll T_c \\ K_c(\varepsilon_\tau) = 0, elsewhere \end{cases} \quad (23)$$

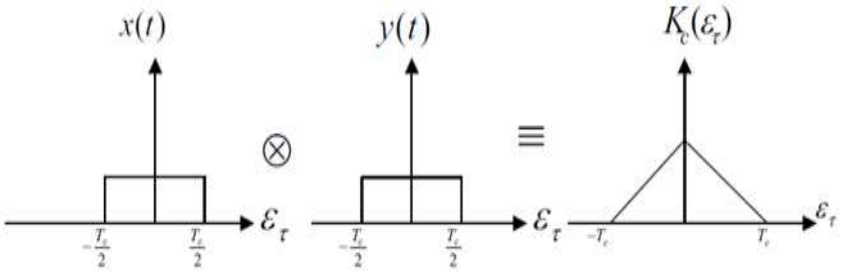

Figure 7. Correlation Process [edited by Authors]

As seen in the figure 7 above the correlation process, when x(t), represents the code rect (t) wave, and y(t) the local generated code, replica and shifted t_0, rect(t-t_0) , are convoluted with each other the form the correlator function , $K_c(\varepsilon_\tau)$, with twice the time interval than any one of them, but if the code is not rectangular waveform, the autocorrelation will be different , in the simulation Matlab program, BOC(binary offset carrier) signals are used , their power spectrum is different , it provides spectral isolation and leads to a significant improvements in terms of tracking and multipath mitigation, a full demonstration of BOC signals are presented in[Macabiau, ION NTM,2005], from this reference we have taken the following BOC equations:

$$G_{BOC}(f) = \frac{1}{T_c}\left(\frac{\sin\left(\frac{\pi f T_c}{n}\right)\sin\left(\pi f T_c\right)}{\pi f \cos\left(\frac{\pi f T_c}{n}\right)}\right)^2 \text{ for the sine phased even n} \quad (24)$$

$$G_{BOC}(f) = \frac{1}{T_c}\left(\frac{\sin\left(\frac{\pi f T_c}{n}\right)\cos\left(\pi f T_c\right)}{\pi f \cos\left(\frac{\pi f T_c}{n}\right)}\right)^2 \text{ for the sine phased odd n.} \quad (25)$$

According to the reference above, both BOC (1,1) and BOC (2,2) are both even, for BOC (p, q)

$f_s = p.1.023MHz$ and $f_c = q.1.023MHz$, then $n = 2\frac{f_s}{f_c} = 2\frac{p}{q}$, if n is even, Equation 19 will be used.

And the result will be calculated by a sub function of the program

Then it can be demonstrated that: $V_e(n) = \frac{A^2}{4}.\left(2 - \frac{C_s}{T_c}\right).\frac{2\varepsilon_\tau}{T_c}$, which is linear discriminator in ε_τ and non-coherent.

4.3 Coherent DLL/Code Tracking Interfering/ Multipath Error

It is the second type of the DLL loops that is dependent on the phase error also, it uses the early minus late correlator, as illustrated in Figure 8 below:

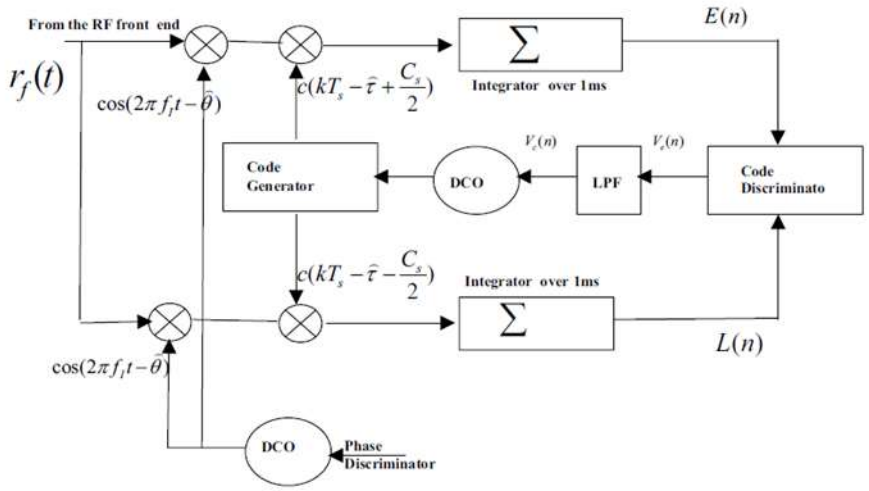

Figure 8. Coherent DLL Loop [edited by Authors]

$$E(n) = \frac{A_0}{2}.K_{cf}.\left(\varepsilon_\tau + \frac{C_s}{2}\right) + \frac{A_1}{2}.K_{cf}.\left(\varepsilon_\tau + \frac{C_s}{2} + \Delta\tau\right).\cos(\Delta\theta) \quad (26)$$

$$L(n) = \frac{A_0}{2}.K_{cf}.\left(\varepsilon_\tau - \frac{C_s}{2}\right) + \frac{A_1}{2}K_{cf}.\left(\varepsilon_\tau - \frac{C_s}{2} + \Delta\tau\right).\cos(\Delta\theta) \quad (27)$$

Early - minus - Late discriminator assuming ε_τ=0 will be

$$V_e(n) = E(n) - L(n)$$

$$V_e(n) = \frac{A_0}{2}.K_{cf}.\left(\varepsilon_\tau + \frac{C_s}{2}\right) - \frac{A_0}{2}.K_{cf}.\left(\varepsilon_\tau - \frac{C_s}{2}\right) + \left(\frac{A_1}{2}.K_{cf}.\left(\varepsilon_\tau + \frac{C_s}{2} + \Delta\tau\right) - \frac{A_1}{2}K_{cf}.\left(\varepsilon_\tau - \frac{C_s}{2} + \Delta\tau\right)\right).\cos(\Delta\theta) \quad (28)$$

If we set:

$$V(\varepsilon_\tau) = K_{cf}.\left(\varepsilon_\tau + \frac{C_s}{2}\right) - K_{cf}.\left(\varepsilon_\tau - \frac{C_s}{2}\right)$$

Then;

$$V(\varepsilon_\tau) = \frac{A_0}{2}.V(\varepsilon_\tau) + \frac{A_1}{2}.V(\varepsilon_\tau + \Delta\tau).\cos(\Delta\theta) = 0 \quad (29)$$

A stable Lock point will be when $V_e(n) = 0$, then $\frac{A_0}{2}.V(\varepsilon_\tau) + \frac{A_1}{2}.V(\varepsilon_\tau + \Delta\tau).\cos(\Delta\theta) = 0$

If $C_s = T_c$, then no more steady point. Then $\alpha = \frac{A_1}{A_0} \leq 1$, is the relative amplitude,

$\Delta\tau \geq 0$: should be positive because there is no delay comes before the LOS signal arrive, LOS signal comes first directly to the antenna, then after the reflected waves follow it. Then the cross point occurs when :

$$V(\varepsilon_\tau) = -V(\varepsilon_\tau + \Delta\tau).\cos(\Delta\theta)\ , in\ the\ interval\ \left[-\frac{C_s}{2}, \frac{C_s}{2}\right]$$

Looking for the zero crossing of the discriminator function is the goal of the Matlab programming, at the envelope then can be resolved to beas close as the following theorectical shape in fugure 9 below:

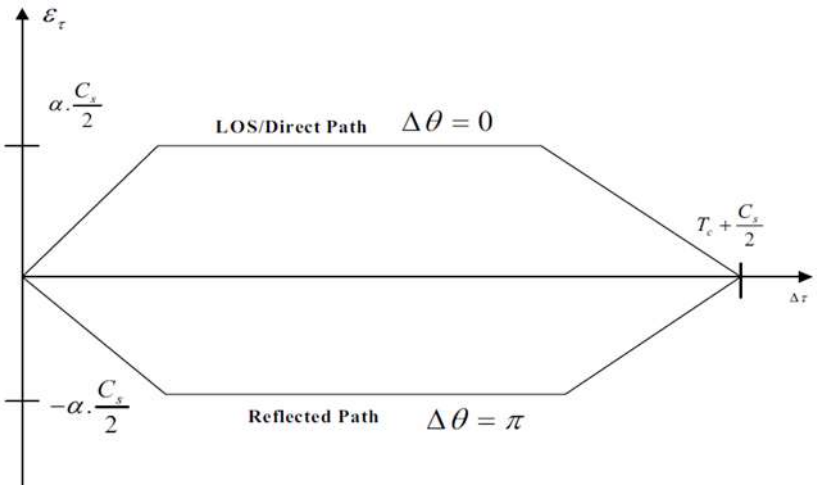

Figure 9. Code Error Envelope of the Multipath [edited by Authors]

5 CODE /PHASE INTERFERING/ MULTIPATH ERROR ENVELOPES ALGORITHMS

Figure 10 below shows the algorithm of the error finding function, it can work properly if there is one zero-crossing point of the discriminator with taw axis, its function is to find the zero crossing points of the discriminator with the τ axis.

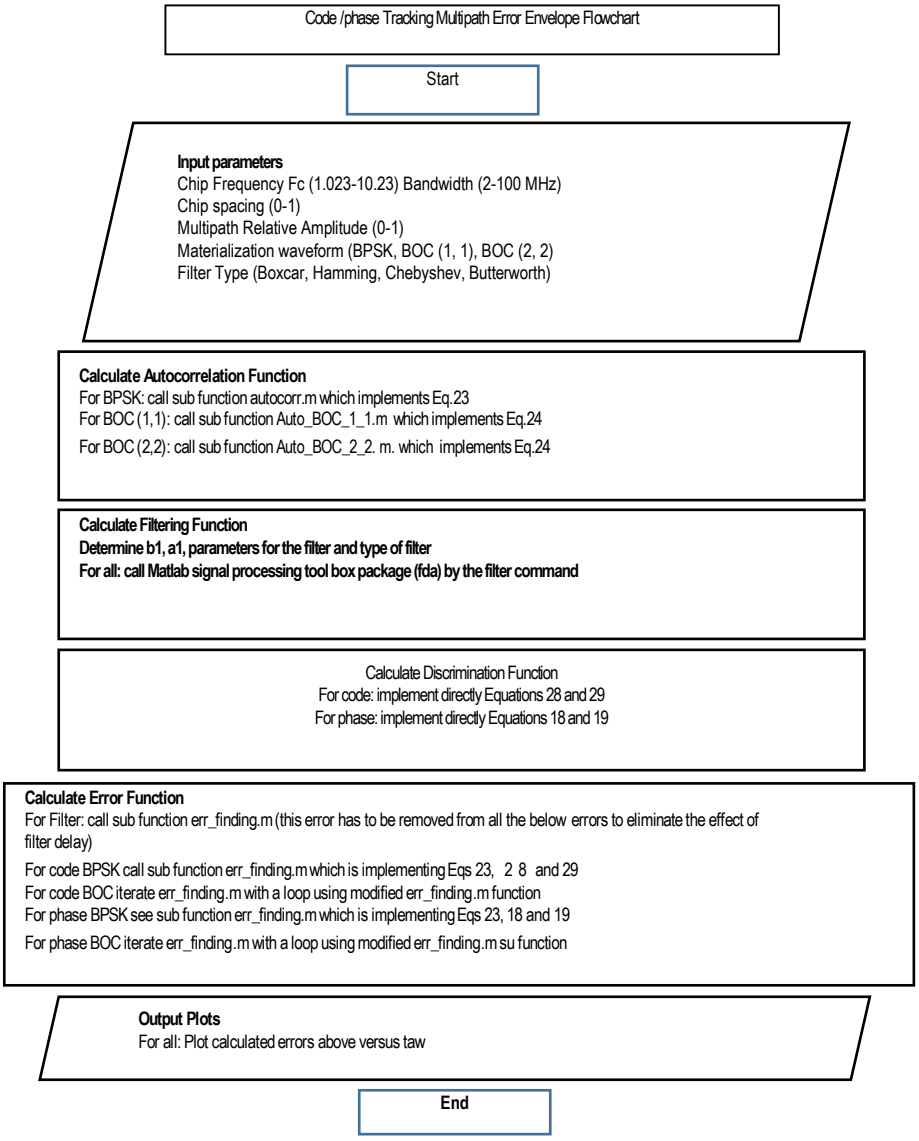

Figure 10. Error finding function and envelope error flowchart [edited by Authors]

6 COMPARISON WITH SIMILAR TECHNIQUES

Actually, our software was validated against similar software done by a worldwide publication paper submitted by Dr. Braasch [Braasch, ION 59th, 2003]. He has used 4 cases of interest in the carrier-phase multipath error envelope:

- Standard correlator spacing (Cs=1), with Relative amplitude (M/D) =-2dB.
- Narrow correlator spacing (Cs=0.1), with Relative amplitude (M/D) =-10dB.
- Standard correlator spacing (Cs=1), with Relative amplitude (M/D) =-2dB.
- Narrow correlator spacing (Cs=0.1), with Relative amplitude (M/D) =-10dB.

In which M/D: is the Multipath to Direct ratio in dB, but we have converted his M/D in dB values to relative ratios under the assumption that Braasch had used:

$$\frac{M}{D}(dB) = 10\ log\left(\frac{A_1}{A_0}\right)^2,\ So,\ \frac{A_1}{A_0} = 10\left[\frac{\frac{M}{D}(dB)}{2*10}\right] \qquad (30)$$

M: is the Multipath reflected signal amplitude, this is Equivalent to 1 A in our notes and D: is the direct signal amplitude, this is equivalent to 0 A in our notes. So, for M/D = -2 dB, A1/A0 =0.7943 and for M/D = -10 dB, A1/A0 =0.3162 to be applied in our software, figure 11 below, and comparison fellows.

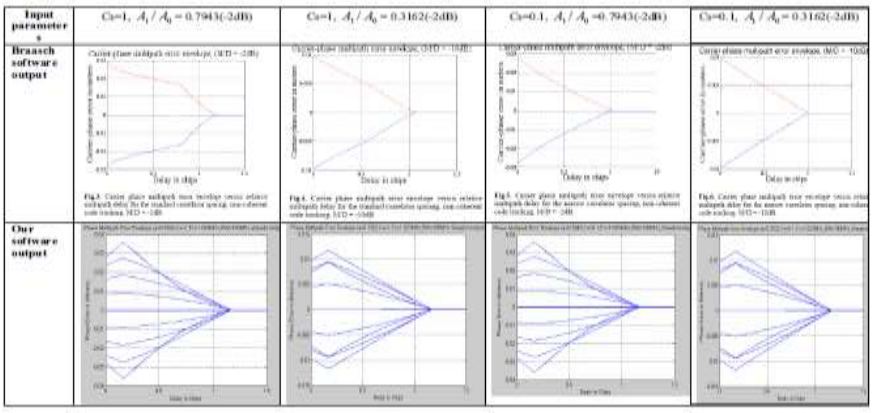

Figure 11. Comparison with similar Software [edited by Authors]

Similarities: Nearly the same output in terms of envelope shape, that's both, have decreasing error with increasing in taw. In addition, both has the same maximum carrier-phase error for the same input parameters taking onto account our software plots more than one curve. Differences: The knee point takes occur at taw = 0.8 chips in Braasch curves, but in ours at taw =0.2 chips, and as chip spacing decreases his curves goes smoothly, but ours still has the same knee at the taw. Justifications: It could be that Braash's curves are plotted according to the approximation formulas not the exact ones that we have used.

7 FINAL RESULT ANALYSIS

7.1. Chip spacing and relative amplitude

The software could be used to any values, but we have taken into account the following parameters assumptions: Varying the chip spacing into two values for the BOC (n, n) and BPSK waveforms: In which both Standard Correlators Cs =0.3, and Narrow correlators Cs=0.1. and the relative amplitude value: α =0.1, in which the first assumption was chosen to be comparable with the other studies and to be compatible with the existing correlators.

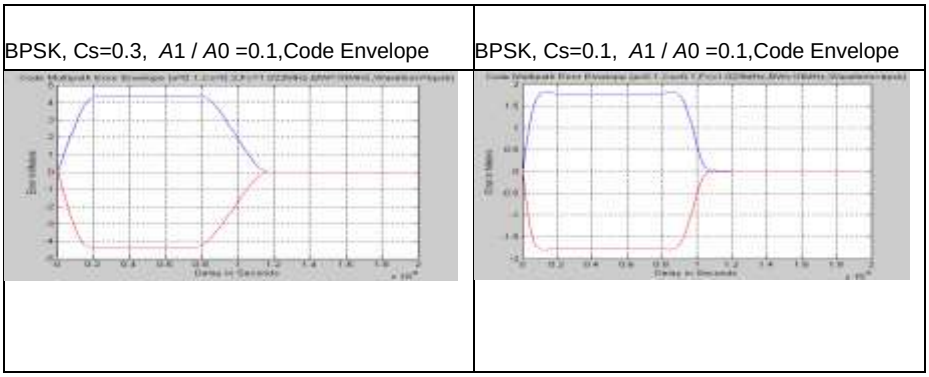

Figure 12. BPSK, code multipath error envelopes [edited by Authors]

Results analysis: Using the BPSAK waveforms, figure 12 above, the chip spacing and the relative amplitude are the key factors in multipath error reduction, when they decreased, the multipath error decrease as shown in the figure 12 above, the Reduction of 0.2 chip spacing (from 0.3 to 0.1) causes the multipath error to be decreased to more than the half.

7.2Materialization waveform type: BPSK, BOC (1,1), and BOC (2,2)

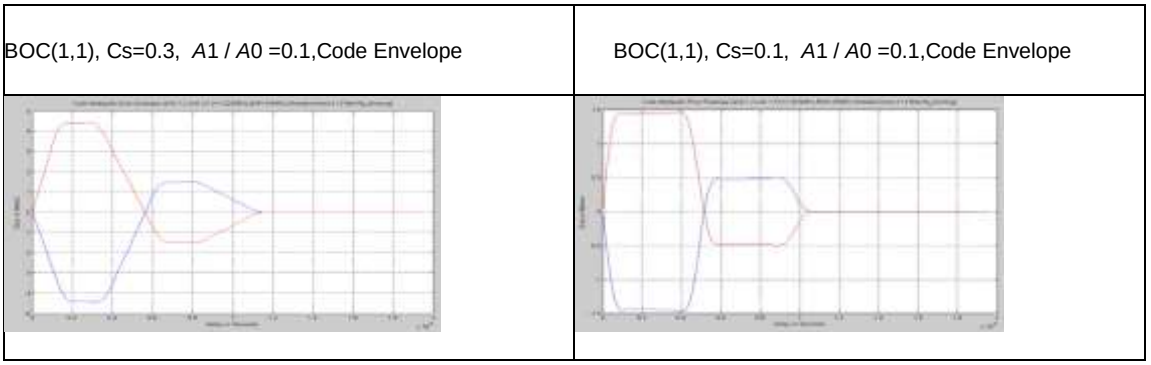

Figure 13. BOC (1,1), code multipath error envelopes [edited by Authors]

Results analysis: Using the BOC (1,1) waveforms, as well as BPSK, the chip spacing and the relative amplitude are the key factors in multipath error reduction, when they are decreased, the multipath error decrease as shown in the figure 13 above, the curve starts as BPSK curves then it crosses the zero in nearly Cs/2, then ends as the BPSK curve again. The reduction of 0.2 chip spacing (from 0.3 to 0.1) causes the multipath error to be decreased to more than one half, also the same can be said for the relative amplitude knowing that the relative amplitude is not controllable factor. The multipath error nearly negligible after the (1) chip delay.

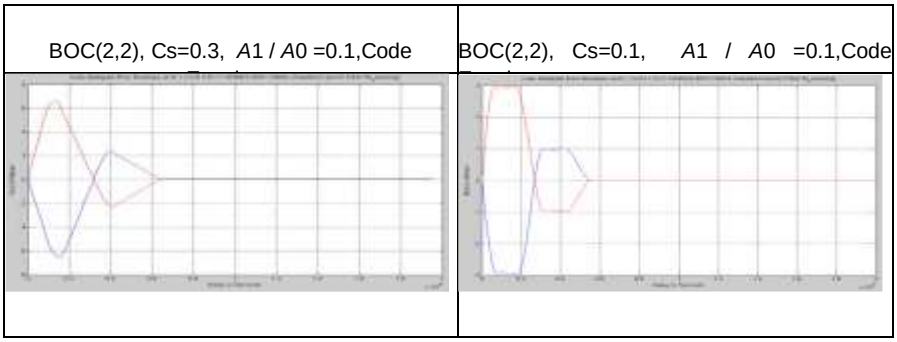

Figure 14. BOC (2,2), code multipath error envelopes

Results analysis: Using the BOC (2,2) waveforms, as well as BPSK and BOC (1,1), the chip spacing and the relative amplitude are the key factors in multipath error reduction, when they decreased, the multipath error decrease as shown in the figure above, However, Reduction of 0.2 chip spacing (from 0.3 to 0.1) causes the multipath error to be decreased to more than the half. The multipath error nearly negligible after the (0.5) chip delay. In addition, the error envelope consists of two parts: the first one overlaid the first half of the affected chip delay with a value near to the achieved one in BPSK, but during the second half period the error is reduced to less than the half for all selected parameters, and this the improvement added by the BOC signals in general.

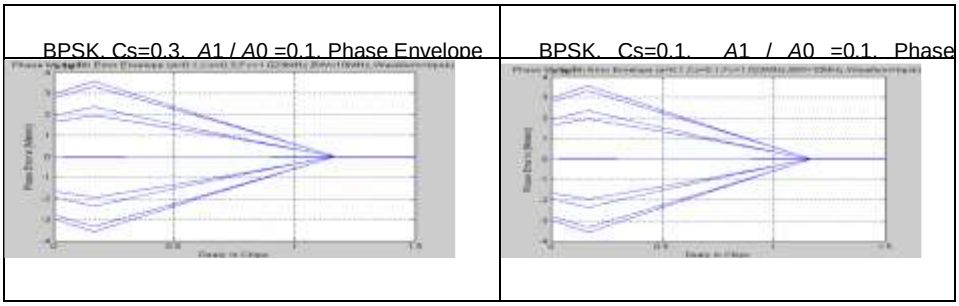

Figure 15. BPSK, phase multipath error envelopes

Results analysis: Using the BPSK waveforms, the relative amplitude is the key factors in multipath error reduction, when it decreased, the multipath error decrease as shown in the figure 15 above, but the chip spacing no more has influence on the multipath error reduction in the phase measurement. The multipath error nearly negligible after the (1) chip delay. The multipath error is less than 1 cm in its highest value, the curve as mentioned previously has a knee (change) around taw = 0.2, then it decreases dramatically towards the zero-crossing point at 1.2 chip delay.

7.3. Filter type Impact

In order to show the filter type impact, we have chosen 4 types of filters. Once the filter delay is known, then it can be removed. figure 16 below.

Final delay = the propagation delay (pseudorange) + the multipath delay - filter delay

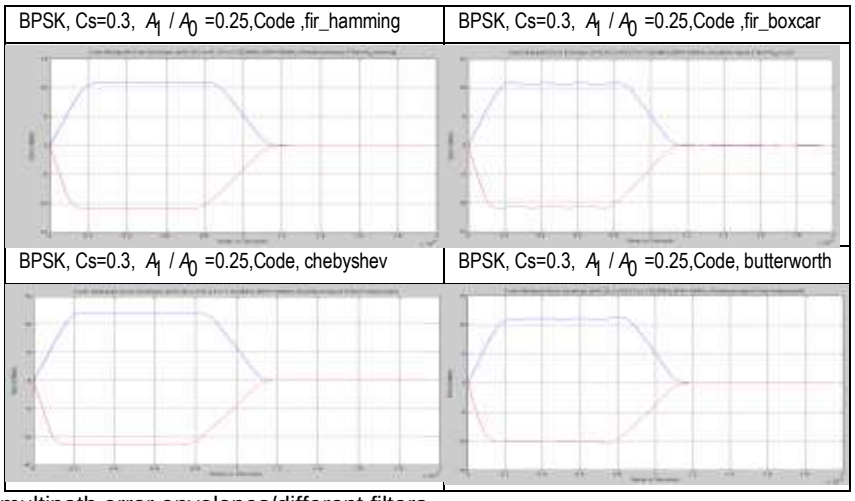

Figure 16. BPSK, code multipath error envelopes/different filters

CONCLUSIONS

The developed new software in Matlab language which was based on the theoretical bases of the signal processing of the receiver , was validated and tested, then it was applied as a simulating tool for the key factors that control the multipath error in the tracking loops, a new BOC signals was implemented in the software for the code tracking loops, with different types of filters. The relative amplitude is the key factor in decreasing the multipath error in the phase tracking error. The future BOC (2,2) waveform impacts the multipath error in such a way that has the best performance among all, BOC (1,1) has better performance than the currently used BPSK. The increase of bandwidth causes a decrease in the multipath error to a certain limit. The type of filter used affects the multipath envelope with ripples. Finally, the software is capable to be modified and improved for more purposes.

REFERENCES

[1] ICAO Annex 10, Volume I, Aeronautical Telecommunications, (2002), Amendment 77, appendix B-89, and Table B-71, B-89.

[2] RTCA DO-245A, *Minimum Aviation System Performance Standards for The Local Area Augmentation System (LAAS)*, (2004), sec 3.3.2.15 Table B-2-2

[3] ICAO Annex 10, Volume I, Aeronautical *Telecommunications,* (2018), Amendment 91, GBAS strategy, section 7.1.2.1, and section 3.3.14

[4] G. Rotondo, (2017), "*Processing and Integrity of DC/DF GBAS for CAT II/III Operations. Signal and Image processing. INPT*", NN: 2016INPT0130, Toulouse, France.

[5] A. Alhosban, (2020), *Navigation Warfare (NAVWAR); Balancing for Position in Space GPS Vs Galileo*, Hadmernok Journal, pp: 163-177, Budapest, Hungary.

[6] President of USA, Executive Order on Strengthening National Resilience through Responsible Use of PNT Services, 2020, website: www.transportation.gov, downloaded on 27 Sep. 2021. Link: https://www.transportation.gov/sites/dot.gov/files/2020-

02/Executive%20Order%20on%20Strengthening%20National%20Resilience%20through%20Responsible%20Use%20of%20Positioning.pdf

[7] B. JW (2001), "*Binary offset carrier modulations for radio navigation*". Navigation 48(4):227–246

[8] Galileo I, (2008) "*Galileo open service, signal in space interface control document*", European space agency/European GNSS supervisory authority.

[9] J. Ma, Y. Yang, H. Li and J. Li, (2020), "*FH-BOC: generalized low-ambiguity anti-interference spread spectrum modulation based on frequency-hopping binary offset carrier*", GPS Solutions (2020) 24:70, https://doi.org/10.1007/s10291-020-00982-3.

[10] X. Zhao, X. Huang, Z. Liu, Z. Xiao, and G. Sun, (2021), "*Improved MBOC modulations based on periodic offset subcarrier, Institute of Engineering and Technology (IET)*", WILEY, DOI: 10.1049/cmu2.12195.

[11] A. Alhosban, (2019), "*Electronic Warfare in NAVWAR: Impact of Electronic Attacks on GNSS / GBAS Approach Service Types C and D Landing systems and their proposed Electronic Protection Measures (EPM)*," Hadmérnök, vol. 14, no. 2, pp. 238–255.

[12] S. Monrocq and J. Arethens, (2003), "*Error Models for Precision Landing with GBAS Using New GNSS Signals*", ION GPS/GNSS, Portland, OR

[13] Braasch, (2002), "*LAAS Integrated Multipath Antenna*", Institute of Navigation ION GPS, VA, USA.

[14] Jean-Pierre (2003), "*Error Models for precision landing using new GNSS signals"*, ION GPS/GNSS, VA, USA.

[15] Alison K. Brown and Ben Mathews, (2005), ION GNSS, Working Group Meetings the18th, ION, VA, USA.

[16] B. Eissfeller, G. Ameres, V. Kropp, D. Sanroma, (2007), "*Performance of GPS, GLONASS and Galileo*", ION, Research gate website: https://www.researchgate.net/search.Search.html?type=publication&query=Performance%20of%20GPS,%20GLONASS%20and%20Galileo , downloaded on the 10 Oct 2021.

[17] Tong P, Yang X, Yang Y, Liu W, Wu P. Multi-UAV Collaborative Absolute Vision Positioning and Navigation: A Survey and Discussion. Drones. 2023; 7(4):261. https://doi.org/10.3390/drones7040261

DOI: https://doi.org/10.15379/ijmst.v10i3.1554

This is an open access article licensed under the terms of the Creative Commons Attribution Non-Commercial License (http://creativecommons.org/licenses/by-nc/3.0/), which permits unrestricted, non-commercial use, distribution and reproduction in any medium, provided the work is properly cited.